CENOZOIC STRESS FIELD EVOLUTION IN THE BAIKAL RIFT ZONE

ÉVOLUTION DU CHAMP DE CONTRAINTE CÉNOZOÏQUE DANS LE RIFT DU BAÏKAL

Vladimir A. SAN'KOV, Andrei I. MIROSHNICHENKO, Kirill G. LEVI, Andrei LUKHNEV, Alexandre I. MELNIKOV and Damien DELVAUX

SAN'KOV, V.A., MIROSHNICHENKO, A.I., LEVI,K.G., LUKHNEV, A., MELNIKOV, A.I. & DELVAUX, D. (1997). — Cenozoic stress field evolution in the Baikal Rift Zone. [*Évolution du champ de contrainte cénozoïque dans le rift du Baïkal*]. — *Bull. Centre Rech. Elf Explor. Prod.*, **21**, 2, 435-455, 10 fig. ; Pau, December 29, 1997. — ISSN : 1279-8215. CODEN : BCREDP.

L'étude détaillée des structures cénozoïques dans la zone de rift du Baïkal montre la présence conjointe de structures extensives (failles normales) et compressives (failles décrochantes, chevauchantes et plissements). L'analyse microstructurale des structures cassantes et l'inversion des données de faille avec stries pour en déduire les tenseurs réduits de contrainte ont permis de reconstruire les champs de contrainte cénozoïque de la zone de rift du Baïkal. La présence de deux types différents de champ de contrainte dans l'évolution spatio-temporelle de la zone de rift du Baïkal est établie : système en extension (« type rift ») et système décrochant à compressif (« type Asie Centrale »). Le champ de contrainte actuel est reconstruit à partir de l'inversion des données de mécanisme au foyer des tremblements de terre. La majorité de la zone de rift du Baïkal est actuellement en extension avec un S_{hmin} orienté NW-SE, tandis que la partie sud-ouest de la zone de rift (bassin de Tunka) est soumise à un régime transpressif.

Le modèle classique d'évolution de la zone de rift du Baïkal en deux étapes est réinterprété en fonction de la fluctuation spatio-temporelle du champ de contrainte. L'évolution progressive du champ de contrainte d'un régime transpressif au stade initial de riftogenèse, à un régime extensif pendant le Quaternaire est mise en évidence. La direction S_{hmin} reste stable dans une direction NW-SE durant toute cette évolution. Le segment sud-ouest de la zone de rift marque la transition depuis la province en extension de type « rift », jusqu'à la province de Mongolie et d'Altaï, en compression.

Nos résultats suggèrent un mécanisme de riftogenèse impliquant une superposition de forces tectoniques à l'échelle continentale, avec un S_{Hmax} orienté NE-SW, et des forces extensives générées par l'ascension d'un diapir mantellique sous la bordure sud-est du craton sibérien.

Vladimir San'kov, Andrei Miroshnichenko, Kirill Levi, Andrei Lukhnev, Alexandre I.Melnikov, Earth's Crust Institute, SB RAS, 664033, Irkutsk, Russia; e-mail: sankov@earth.crust.irk.ru; Damien Delvaux, Royal Museum of Central Africa, B-3080, Tervuren, Belgium; e-mail: ddelvaux@africamuseum.be . — November 12, 1997.

Mots-clés : Champ contrainte, Cénozoïque, Transpression, Tectonique extension, Rifting, Rift Baïkal.

ABSTRACT

Detailed investigation of Cenozoic structures in the Baikal rift zone (BRZ) revealed the existence of both extensional structures (normal faults) and compressional structures (strike-slip faults, thrusts and folding). Microstructural analysis of brittle structures and stress inversion of fault-slip data permitted the reconstruction of the Cenozoic paleostress field for the central and southwest parts of the BRZ. The presence of two different types of stress field in the spatio-temporal evolution of the BRZ is established: stress tensors of extensional "rift-type" regime and stress tensors of strike-slip to compressional "Central Asian-type" regime. The present-day stress field is reconstructed by stress inversion of earthquake focal mechanism data. Most part of the BRZ is presently in an extensional setting, with NW-trending S_{hmin}, while the southwestern part of the rift zone (Tunka basin) is in a transpressional setting.

The classical two-stage evolution model of the BRZ is interpreted in function of stress field fluctuation in time and space. Regular evolution of the stress field from a strike-slip or transpressional regime in the initial stage of rifting to pure extensional regime in the Quaternary is revealed. The S_{hmin} direction remained stable in a NW-SE orientation during all this evolution. The southwestern segment of the BRZ marks the transition from the "rift-type" extensional stress field, to the compressional stress field of Mongolia and of Altai.

Our results rather suggest a mechanism of Baikal rift formation involving the superposition of continental-scale tectonic forces with NE-trending S_{Hmax} and extensional forces generated by a mantle diapir rising beneath the southeastern boundary of the Siberian Craton.

Keywords: Stress field, Cenozoic, Transpression, Extension tectonics, Rifting, Baikal Rift.

1279-8215/97/0021-0435 $ 4.20

CONTENTS — *TABLE DES MATIÈRES*

INTRODUCTION 436

1. — INVESTIGATION OF CENOZOIC STRESS FIELD IN THE BAIKAL RIFT ZONE — *ÉTUDE DU CHAMP DE CONTRAINTE CÉNOZOÏQUE DU RIFT DU BAÏKAL* 436
   - 1.1. Seismotectonic data — *Données sismotectoniques*
   - 1.2. Structural and kinematic data — *Données structurales et cinématiques* 436

2. — STAGES OF BAIKAL RIFT DEVELOPMENT — *ÉTAPES DU DÉVELOPPEMENT DU RIFT DU BAÏKAL* 436
   - 2.1. Two-stage evolution model — *Modèle d'évolution en deux phases* 437
   - 2.2. Tectonic changes during rifting — *Modifications tectoniques pendant la riftogenèse* 437
     - 2.2.1. Extensional structures — *Structures extensives* 437
     - 2.2.2. Compressional structures — *Structures compressives* 437

3. — REDUCED STRESS TENSOR RECONSTRUCTION — *RECONSTITUTION DU TENSEUR DE CONTRAINTE RÉDUITE* 441

4. — CENOZOIC STRESS FIELD FROM FAULT KINEMATIC DATA — *CHAMP DE CONTRAINTE CÉNOZOÏQUE A PARTIR DE LA CINÉMATIQUE DES FAILLES* 441

5. — PRESENT-DAY STRESS FIELD FROM SEISMOLOGICAL DATA — *CHAMP DE CONTRAINTE ACTUEL A PARTIR DES DONNÉES SISMIQUES* 446

6. — STRESS FIELD EVOLUTION DURING CENOZOIC — *ÉVOLUTON DU CHAMP DE CONTRAINTE PENDANT LE CÉNOZOÏQUE* 446

7. — CONCLUSIONS 447

8. — REFERENCES 449

INTRODUCTION

The Baikal rift zone (BRZ), like the East African, Shanxi (Fen-Wei) and Rio Grande rift systems, is one of the few intracontinental tectonic structures of high seismic activity which is largely under extensional tectonic stress field. The fact that an active rift develops in the central part of the Eurasian continent poses a major question: is this rift an isolated continental structure, or is it part of the world system of rifts and spreading ridges? The BRZ is considered by MILANOVSKY (1976) at an initial stage of evolution towards the formation of mid-oceanic ridges. ZOBACK (1992) shows that most of the intracontinental areas (including Eurasia) are characterized by dominantly compressional stresses. This poses a new question: how do rifts develop in continental areas which are largely submitted to compressional stresses ?

The main problems addressed in this paper are to determine whether the stress state in the BRZ remained stable during Cenozoic or if it changed with time. This will contribute to the understanding of the mechanism of rifting. In particular, it will bring new elements to determine whether rifting is the product of a local process (active rifting), or if it is the effect of external tectonic stresses applied to the Eurasian plate by the India-Asia collision and the Pacific-Asia subduction (passive rifting).

1. — INVESTIGATION OF CENOZOIC STRESS FIELD IN THE BAIKAL RIFT ZONE

1.1. SEISMOTECTONIC DATA

The first seismotectonic data on the state of stresses in the Baikal rift zone has been published by VVEDENSKAYA & BALAKINA (1960). Shortly after, MISHARINA (1964, 1972) presented the first compilation of focal mechanism data and showed that the present stress field in the central part of the BRZ is characterized by NW-trending horizontal principal extension (S_{hmin}) and vertical principal compression (normal faulting mechanism). Further research allowed to specify the boundaries of the areas subjected to the "rift" type extensional stresses and to precise the distribution of focal mechanism types in the BRZ and surrounding area (MISHARINA & SOLONENKO, 1977, 1981a, 1981b; MISHARINA *et al.*, 1983, 1985).

By modelling a small number of teleseisms from the BRZ, DOSER (1991) concluded that about one third of the teleseisms in the BRZ have a strike-slip mechanism. She also computed a regional stress tensor from the focal mechanisms obtained. Her conclusions, however, are not entirely supported by the focal mechanisms data obtained from the regional network of seismic stations (SOLONENKO, 1993; SOLONENKO *et al.*, 1997).

The distribution of compressional (P) and extensional (T) geometrical axes of focal mechanisms in the BRZ, established by SOLONENKO (1993), presents a symmetrical pattern along trend, with a symmetry axis situated at the northern end of Lake Baikal. Using detailed seismological data from the North Muya geodynamic polygon, DÉVERCHÈRE *et al.* (1993) computed a local stress tensor with 36 focal mechanisms of various magnitudes, from a depth ranging between 5 and 15 km.

The most comprehensive compilation of focal mechanism data has been presented by SOLONENKO *et al.* (1997). They studied the statistical distribution of P and T axes of more than 300 focal mechanisms and showed that the stress field changes from extensional "rift" type in central part of the BRZ, to strike-slip and compressive "Central-Asian" type at both extremities of the BRZ: the East Sayan massif and West Mongolia to the southwest, and the Stanovoy Belt to the northeast. Based on a critical revision of the database of SOLONENKO *et al.* (1997), PETIT *et al.* (1996) computed the present-day stress field in 15 different sectors of the BRZ, by stress tensor inversion of 332 focal mechanisms.

1.2. STRUCTURAL AND KINEMATIC DATA

In the 1960's, SHERMAN and co-workers initiated paleostress investigations in the BRZ using geological and structural methods. Compilation of the results obtained are presented by SHERMAN & DNEPROVSKY (1989) and SHERMAN (1992). They reveal that normal faulting regime with NW-trending S_{hmin} is typical for the central part of the BRZ. Local stress fields, with principal axes of extension and compression both subhorizontal and trending respectively NW and NE, are dominant in the northeastern and southwestern segments of the BRZ. In consequence, the central part of the BRZ is characterised by extensional stress field and its extremities, by strike-slip stress field. Through comparative analysis of ancient and recent stress field in the BRZ, SHERMAN & DNEPROVSKY (1989) concluded that the regional stress field has been stable during the second half of the Cenozoic. These authors used the procedure of GZOVSKY (1975) and NIKOLAEV (1977), which allows to reconstruct only the geometrical principal axes of compression and extension, from a statistical analysis of joint and fracture planes. It has to be noted that this method does not permit reduced stress tensor inversion.

From detailed structural analysis in the East Sayan massif, RUZHICH (1972) concluded that the stress field changed with time in the southwestern segment of the BRZ, with a clockwise rotation of S_{Hmax} directions from a N-S trend in the Mesozoic, to a NE-trend in the Cenozoic. Based on fault kinematic data for northeastern segment of the BRZ, VISLAVNICH (1982) suggested that movement along major faults changed from strike-slip to normal faulting during rifting. He concluded that this change is related to a modification of stress field with time in the area comprised between the Upper Angara and Muya rivers.

One of the first attempts to assess the temporal changes of stress field in the BRZ was undertaken by RASSKAZOV (in SHERMAN *et al.*, 1984). Applying the technique proposed by GZOVSKY (1975) for the study of joints in basalts and orientation of dikes in the Udokan basalt field, he revealed that the principal extension axes rotated clockwise from a NW trend at the early stages of volcanism (Late Miocene - Middle Pliocene), to a NE trend at the final stage (about 2 Ma ago). The temporal variations of the stress field in the region of volcanic activity are interpreted by RASSKAZOV (1993) as caused by changes in the crustal dynamics during volcanic and tectonic activity.

From the strike analysis of dated basalt dikes in the Tunka basin and adjacent mountain ranges (SW part of BRZ, Fig. 1), RASSKAZOV (1993) concluded that the direction of principal extension (S_{hmin}) changed from a NW trend in the Middle Miocene, to a sublatitudinal one in the Late Pleistocene. However, a comparison of S_{hmin} directions obtained from Early-Middle Miocene dikes and those reconstructed from fracture analysis in the same rocks of the Main Sayan fault shows that the S_{hmin} directions changed from a NW trend during the peak of volcanism activity, to a NE trend in the post-volcanic stage.

Detailed studies of Cenozoic faulting and seismicity in the North Muya geodynamic polygon (central part of the northeastern segment of the BRZ), have been carried out by SAN'KOV *et al.* (1991). It allowed the recognition of three different strain and stress stages in this area during the Cenozoic: Early Cenozoic, Upper Pleistocene-Holocene and Present-day. The Early Cenozoic stage is characterized by strike-slip stress field with NW-trending S_{hmin} and NE-trending S_{Hmax}. In the Pleistocene-Holocene, transtensional type of stress field is predominant. Extensional type of stress field is typical for the Present-day, but S_{hmin} trajectories deviate from the typical NW trend, probably due to the influence of structural heterogeneities (SAN'KOV *et al.*, 1991).

DNEPROVSKY & SAN'KOV (1992) concluded that at least two major stress stages can be differentiated during the development of the BRZ. The early stage is characterized by the predominance of strike-slip stress fields whereas extensive stress fields are prevalent during the younger stage of rifting. The same conclusion was also reached by DELVAUX *et al.* (1997). In addition, DELVAUX *et al.* (1995) stated the importance of pre-rift tectonic activity in the BRZ, recognising at least four major stress stages related to major tectonic events and ranging from the Early Paleozoic to the Late Mesozoic.

2. — STAGES OF BAIKAL RIFT DEVELOPMENT

2.1. TWO-STAGE EVOLUTION MODEL

The sedimentation rate and the velocity of vertical movements in the BRZ has been reported to vary during rifting (LOGATCHEV & FLORENSOV, 1978; LOGATCHEV, 1993). Fine-grained sediments were accumulating since the Oligocene in slowly subsiding basins, while coarse sediments were deposited with a higher sedimentation rate since the Middle Pliocene, in rapidly subsiding rift basins (KASHIK & MAZILOV, 1994). FLORENSOV (1964) called these two paleogeographic stages of development as "proto-Baikal" and "neo-Baikal" stages. LOGATCHEV *et al.* (1974) named them as "early rift" and "late orogenic" stages and LOGATCHEV & FLORENSOV (1978), as "slow rifting" and "fast rifting" stages. In addition to this major subdivision, evidences have been found that vertical movements in the BRZ were further accelerated in the Late Pleistocene (KULCHITSKY, 1992).

The observed velocity changes of vertical movements were explained by LOGATCHEV & ZORIN (1987) and LOGATCHEV (1993) in a model involving deep-seated rifting dynamics. The first stage of rift development (slow rifting) is related to the uplift of a mantle diapir, starting 30 Ma ago. The second stage (fast rifting) is associated with the arrival, ±3 Ma ago, of the diapir at the base of the crust, and to its lateral expansion. A slightly different explanation is given by DELVAUX *et al.*, (1997), who suggested that the two stages of BRZ development correspond to two major stages of plate-scale crustal stress, with an interaction between external plate-scale stress field, pre-existing lithospheric structures which are reactivated, and local stresses generated by the rising of a mantle diapir.

2.2. TECTONIC CHANGES DURING RIFTING

A wide variety of tectonic structures formed during the Cenozoic development of the BRZ. They comprise extensional structures (normal faults), wrench-faulting structures (strike-slip faults, flower structures), as well as compressive structures (reverse and thrust faults, folds). Their variety, spatial distribution and age of development testify for a complex kinematic behaviour in time and space.

2.2.1. Extensional structures

Normal faults are the major tectonic structures of the BRZ. The major ones are represented by 1000 - 2000 metres high topographic scarps above the lake level. The offset of the pre-rift Cretaceous-Paleogene planation surface between the summits of the rift flanks and the base of Cenozoic sediments in the rift basin ranges from a few hundred to between 7000 and 8000 metres. It is the highest for the Obruchev fault system, which forms all the western flank of the Baikal basin at the foot of the Primorsky rift shoulder. Several segments of the Obruchev fault

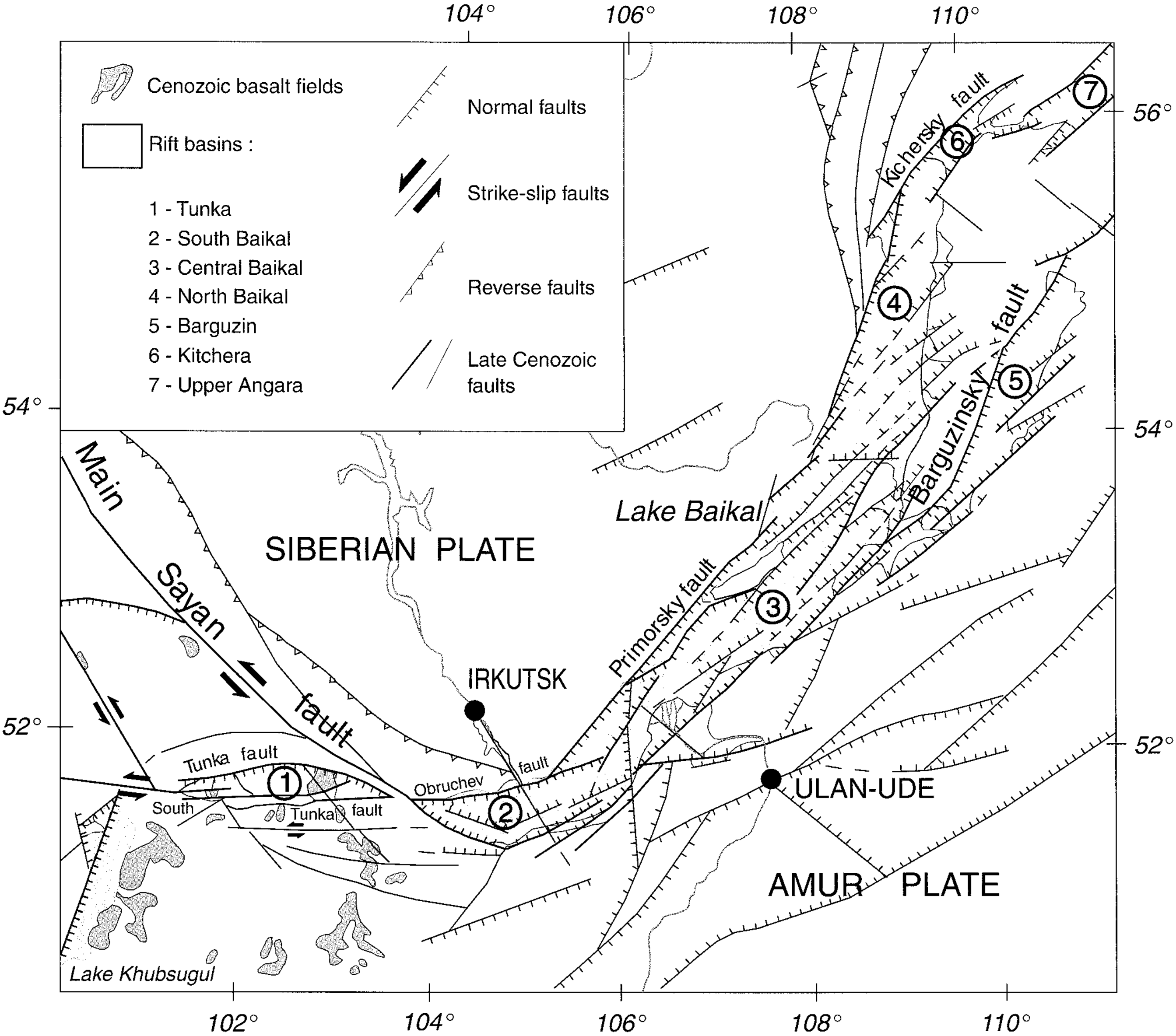

FIGURE 1

Map of the major Late Cenozoic faults of the Baikal rift zone.

Carte des failles majeures d'âge cénozoïque tardif de la zone de rift du Baïkal.

can be observed at the surface (Fig. 2), while others are mainly underwater. In the Olkhon area, the Obruchev fault is splayed into several segments, the major ones being the Primorsky fault (less than 1000 metres displacement) and the Olkhon fault (more than 5000 metres displacement). Fractures with dip-slip slickensides are dominant in the fault plane itself, but oblique and subhorizontal striations and grooves are also observed. *En échelon* faulting is typical for the western side of the Baikal basin, especially along its northeastern segment.

In the southwestern segment of the BRZ, the maximum throw (1500 - 2000 metres) occurs along the Tunka fault, between the Tunka Range and the Tunka depression (Fig. 3). Limited lateral displacements of thalwegs and small rivers suggest the existence of a horizontal component of movement along the Tunka fault. Both vertical and inclined striations and grooves are observed in the fault plane.

West of the North Baikal basin, the Barguzin fault separates the Barguzin Range from the Barguzin basin. It has a normal displacement reaching 2000 metres. *En échelon* fault structure is also typical for both the Barguzin fault and the western border fault of the North Baikal basin.

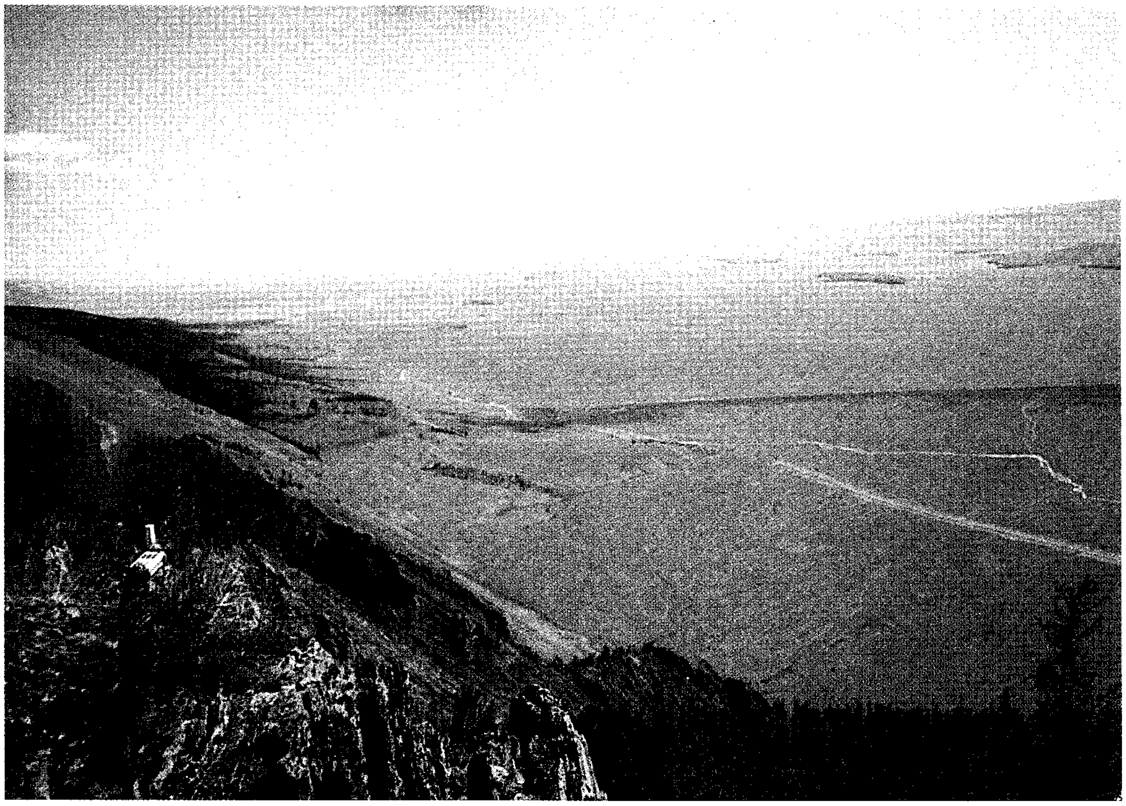

FIGURE 2a
View of the Primorsky fault along the NW side of the Baikal basin, from the top of the fault scarp to the Small Sea and Olkhon Island (Photo by V.A. San'kov).
Vue de la faille de Primorsky le long de la bordure NW du bassin du Baïkal, depuis le sommet de l'escarpement de faille vers la Small Sea et l'île d'Olkhon (Photo V.A.San'kov).

FIGURE 2b
Paleoseismic dislocation along the Primorsky fault (Photo by A.A.Bukharov).
Dislocation paléosismique le long de la faille de Primorsky (Photo A.A.Bukharov).

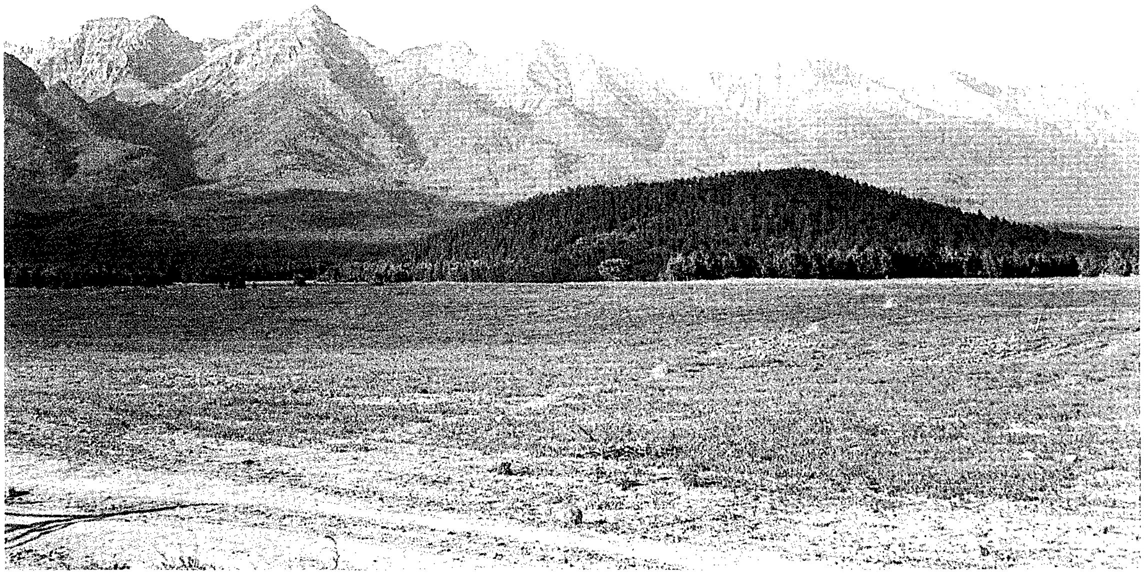

FIGURE 3

View of the Tunka fault which bounds the Tunka basin from the north. A basaltic volcano is in the foreground (Photo by V.A. San'kov).

Vue de la faille de Tunka qui borde le bassin de Tunka au nord. Au premier plan, un volcan basaltique (Photo V.A. San'kov).

FIGURE 4

Dextral displacement of a basaltic dike dated 11.4 Ma, along a gentle fault. The visible horizontal displacement is 8 metres (Photo by V.A. San'kov). Scale: D. Delvaux measuring slickensides.

Déplacement dextre par une petite faille, d'un dyke basaltique daté 11,4 Ma. Le rejet horizontal visible est de 8 mètres (Photo V.A. San'kov). Échelle : D. Delvaux mesurant des stries.

2.2.2. Compressional structures

Along with typical normal faults, Cenozoic compressive structures like thrust faults and folds are common in the south-western part of the BRZ. The formation of such compressive structures in a rift environment requires a special attention. They were named "non-rift structures" because they did not fit into the classical idea that rift forms by extension. Consequently, they were generally not taken into account in the discussion of rifting mechanism. Here, we want to stress the existence of compressional structures in the Tunka and South Baikal basins and along the Main Sayan fault.

Thrust and strike-slip faults

The presence of Cenozoic thrust faults is well known in East Sayan, since RUZHICH *et al.* (1972) found a nice thrust fault in the Tunka Range, displacing a 11.4 Ma Miocene basalt dike (Fig. 4). The thrust faults are located 1400 metres above the Tunka basin floor, suggesting their ancient, most probably pre-Quaternary age. Similar minor thrust faults displacing Miocene basalt dikes were discovered by SAN'KOV & DNEPROVSKY (1987) in the southern flank of the Tunka basin. In the Oka plateau, northwest of the Tunka basin, RASSKAZOV (1990) described a thrust fault displacing a 2.3 Ma basalt layer.

The Main Sayan fault has a sisnistral strike-slip component of displacement of 8 to 11 km, based on major river offset. Paleoseismic dislocations along the southeastern segment of this fault also revealed Late Pleistocene-Holocene strike-slip movements (CHIPIZUBOV *et al.*, 1994).

Recently we observed sisnistral strike-slip displacements along W-E trending segments of the Tunka fault near Kultuk, at the western extremity of Lake Baikal. The amplitudes of Holocene movements in different segments of the fault vary from 3 to 25 metres.

Fractures with subhorizontal slickensides or grooves are frequent along the southern border fault of the Tunka depression. The most spectacular example is a ENE-striking, sinistral strike-slip fault system that displaced sandstones and conglomerate in the western termination of the Tunka depression, near Mondy (Fig. 5). These deposits are not dated, but they are estimated to be Miocene, since they do not contain pebbles of basaltic lava which are known upstream and are of Late Miocene-Pliocene age. Similar strike-slip to oblique-slip faults together with subvertical slipelines are also observed 50 km further east near Nilova-Pustyn, in Late Miocene basalts, dated at 7.57 Ma (in UFIMTSEV, 1996) (Fig. 6a & b).

Folds

The most spectacular examples of Cenozoic compressional structures are long-wavelength folds in the sediments of the South Baikal basin, revealed by seismic profiling (LEVI *et al.*, 1997; VON HAUGWITZ *et al.*, in press). Three major seismostratigraphic units were identified. The lower unit is attributed to the Late Oligocene-Early Pliocene, the intermediate unit to the Late Pliocene-Early Pleistocene and the upper unit to the Middle Pleistocene-Holocene (NIKOLAEV, 1990; HUTCHINSON *et al.*, 1992). The intermediate unit is deformed into long-wavelength folds trending NW-SE, while the upper unit lies undeformed on top. Minor folds with NW-trending axes were also found by VOROPINOV (1961) in the outcropping Miocene-Early Pliocene carbonaceous sediments along the southern shore of the South Baikal basin. This provides good evidence for a compressive deformation in the South Baikal basin in the Late Pliocene-Early Pleistocene. This deformation is compatible with a general NE-SW trending horizontal principal compression.

In the central part of the Tunka depression, LOGATCHEV *et al.* (1974) observed small-scale folds in marls of Miocene-Early Pliocene age, overlain by non-deformed Quaternary deposits. Minor folds were also found in the Plio-Pleistocene volcano-sedimentary formation overlying the Elovsky uplifted basement block, in the middle of the Tunka depression.

In conclusion, the structural data presented above suggest that a Late Cenozoic compressional to strike-slip deformation affected the Tunka and South Baikal basins, at least from the Late Miocene, and up to the Middle Pliocene.

Considering the paleogeographic and stratigraphic data, it seems clear that the tectonic context during rifting changed with time. This contradicts to some extent the views of SHERMAN & DNEPROVSKY (1989) who claimed that the state of crustal stresses in the BRZ remained stable during the Cenozoic.

To make a better link between stress field and tectonic evolution, our work will concentrate on the investigation of paleostress and present stress fields in the Baikal rift zone and their evolution in time and space.

3. — REDUCED STRESS TENSOR RECONSTRUCTION

To characterize the evolution of crustal stress field in the Baikal rift zone during the Cenozoic, reduced stress tensors were reconstructed by inversion of fault kinematic data (fault planes with slip line and slip sense).

The inversion is based on the assumption that slip on a plane occurs in the direction of the maximum resolved shear stress (BOTT, 1959), and that the apparent slip direction on the fault plane can be inferred from frictional grooves or slickensides. According to classical procedures as those developed by ANGELIER & MECHLER (1977), ANGELIER (1989; 1994) and DUNNE & HANCOCK (1994), fault and joint data were inverted to obtain the four parameters of the reduced stress tensor. These are the principal stress axes $\sigma1$ (maximum compression), $\sigma2$ (intermediate compression) and $\sigma3$ (minimum compression) and the ratio of principal stress differences $R = (\sigma2 - \sigma3)/(\sigma1 - \sigma3)$. These parameters are determined using the TENSOR program developed by DELVAUX (1993).

The tensors are classified into different stress regimes and represented graphically as in GUIRAUD *et al.* (1989). Three major stress regimes are distinguished, according to the nature of the vertical stress axes: extensional ($\sigma1$ vertical), strike-slip ($\sigma2$ vertical) and compressional ($\sigma3$ vertical). The stress regime is further classified in function of the stress ratio R: radial extension ($\sigma1$ vertical, $0<R<0.25$), pure extension ($\sigma1$ vertical, $0.25<R<0.75$), transtension ($\sigma1$ vertical, $0.75<R<1$ or $\sigma2$ vertical, $1>R>0.75$), pure strike-slip ($\sigma2$ vertical, $0.75>R>0.25$), transpression ($\sigma2$ vertical, $0.25>R>0$ or $\sigma3$ vertical, $0<R<0.25$), pure compression ($\sigma3$ vertical, $0.25<R<0.75$) and radial compression ($\sigma1$ vertical, $0.75<R<1$). The type of stress regime are also expressed numerically using an index R', ranging from 0.0 to 3.0 and defined as in DELVAUX *et al.* (1997) :

R' = R when $\sigma1$ is vertical (extensional stress regime),

R' = 2-R when $\sigma2$ is vertical (strike-slip stress regime),

R' = 2+R when $\sigma3$ is vertical (compressional stress regime).

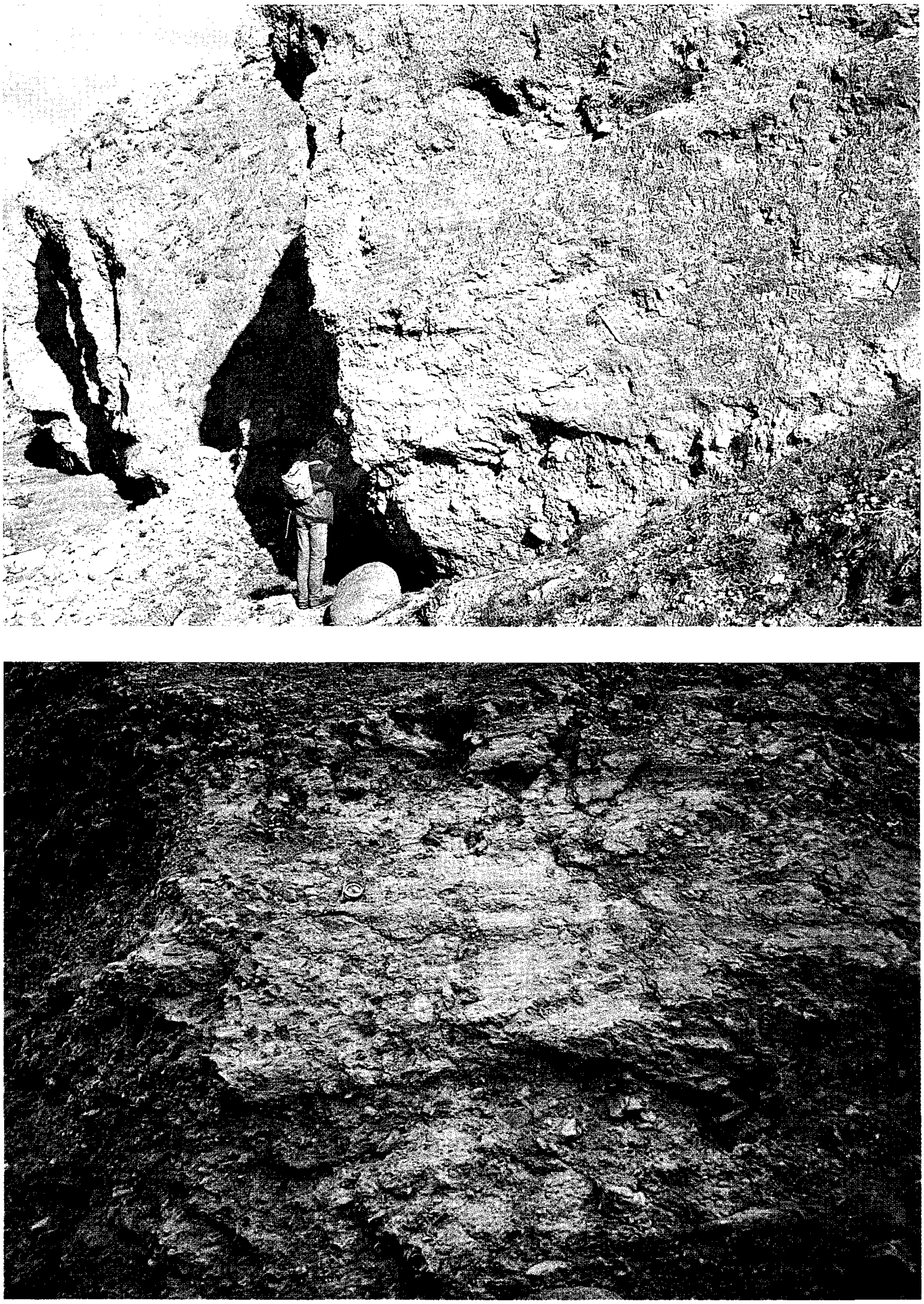

FIGURE 5

E-W trending faults with slickensides in Miocene conglomerates near Mondy (western extremity of Tunka depression). a - general view (Photo by D. Delvaux); b - detail of slickenside showing sinistral movement (Photo by V.A. San'kov).

Failles E-W présentant des stries dans des conglomérats miocènes près de Mondy (extrémité orientale de la dépression de Tunka). a - vue générale (Photo D.Delvaux) ; b - détail d'un plan strié montrant un mouvement senestre (Photo V.A.San'kov).

FIGURE 6

Faults in the Late Miocene basalts dated 7.57 Ma, near Nilova Pustyn (Photos by V.A. San'kov).
a - general view; b - dip-slip slickensides.

Failles dans les basaltes miocène tardif datés 7,57 Ma, près de Nilova Pustyn (Photos V.A.San'kov).
a - vue générale ; b - stries selon la plus grande pente.

4. — CENOZOIC STRESS FIELD FROM FAULT KINEMATIC DATA

To reconstruct the Cenozoic stress field evolution in the BRZ, fault-slip data were obtained from more that 200 sites located in the Baikal, Barguzin, Tunka and Kitchera basins. Fault data were analysed both in pre-Cenozoic basement rocks (mostly crystalline) and in rift sediments and volcanics. When working in pre-Cenozoic basement, measurements were generally made in young fault zones characterized by a marked morphological scarp. If measurement sites show evidence for polyphase brittle fracturing, only fractures from the latest stage of deformation were used. In addition, Cenozoic fractures are generally characterized by poorly consolidated fault breccia with only thin mineral coatings such as calcite and zeolite. They also frequently have typical clay gouge with slickensides impressed on clay. To constrain the maximum age of faulting, much attention was paid to the analysis of tectonic fracturing in Cenozoic sediments, dated basaltic volcanics and products of the Late Cretaceous-Paleogene weathering crust.

Given in Appendix 1 are the computed reduced stress-tensors, referring to the Cenozoic. They were carefully selected from a large data set on tectonic fracturing of the Baikal rift, available to the authors. In a first approximation all the stress tensors can formally be divided into two groups. As the main Cenozoic tectonic regime is extensional, all the stress-tensors, with subvertical principal compression were grouped in a first set. The remaining tensors, with subhorizontal principal compression, are grouped in a second set.

Tensors from the first population were obtained from 47 sites (Fig. 7). Most of them are of pure extensional to transtensional type but a few of them have a radial extensive regime in the South Baikal, Central Baikal and Kitchera basins. The second

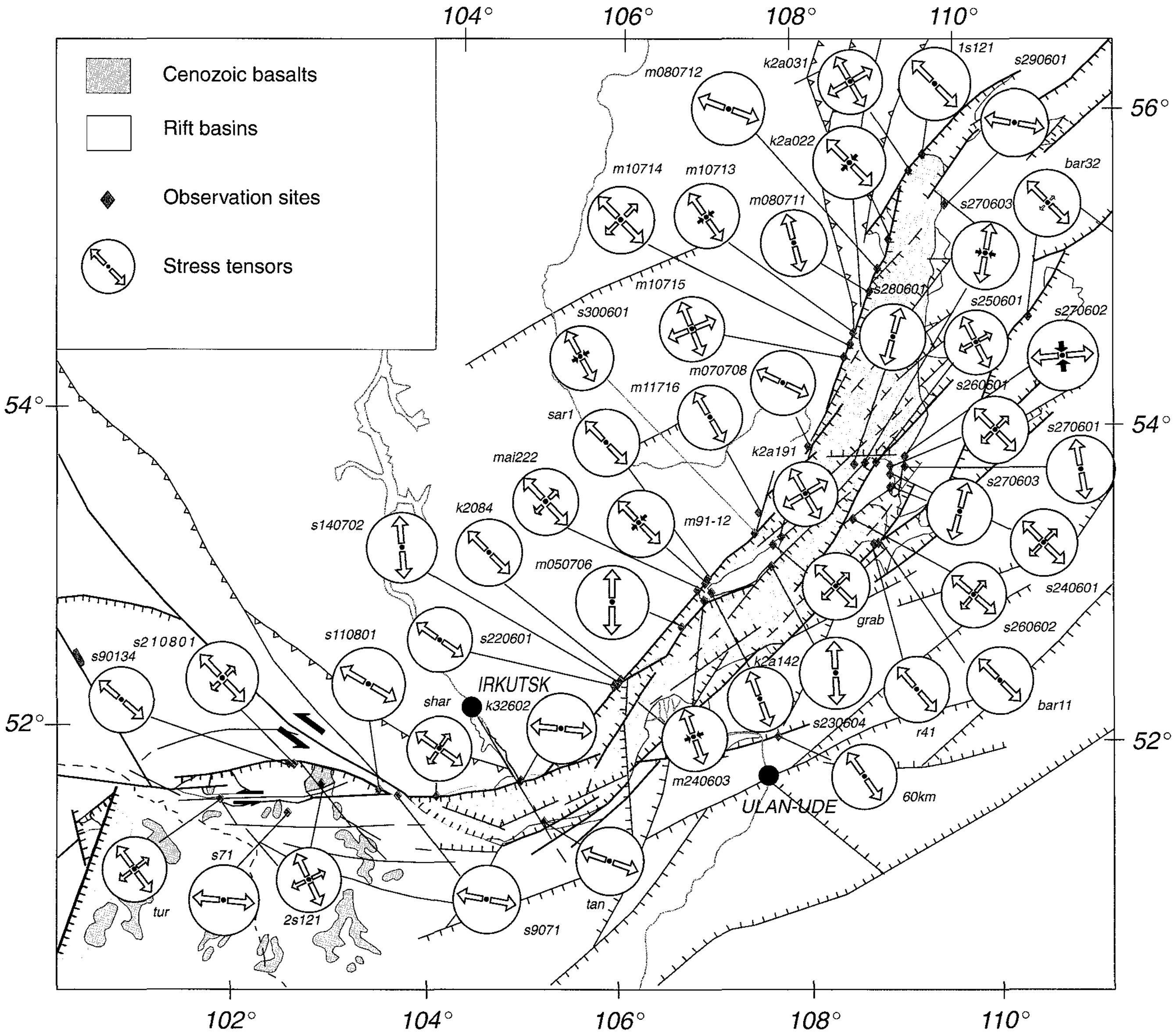

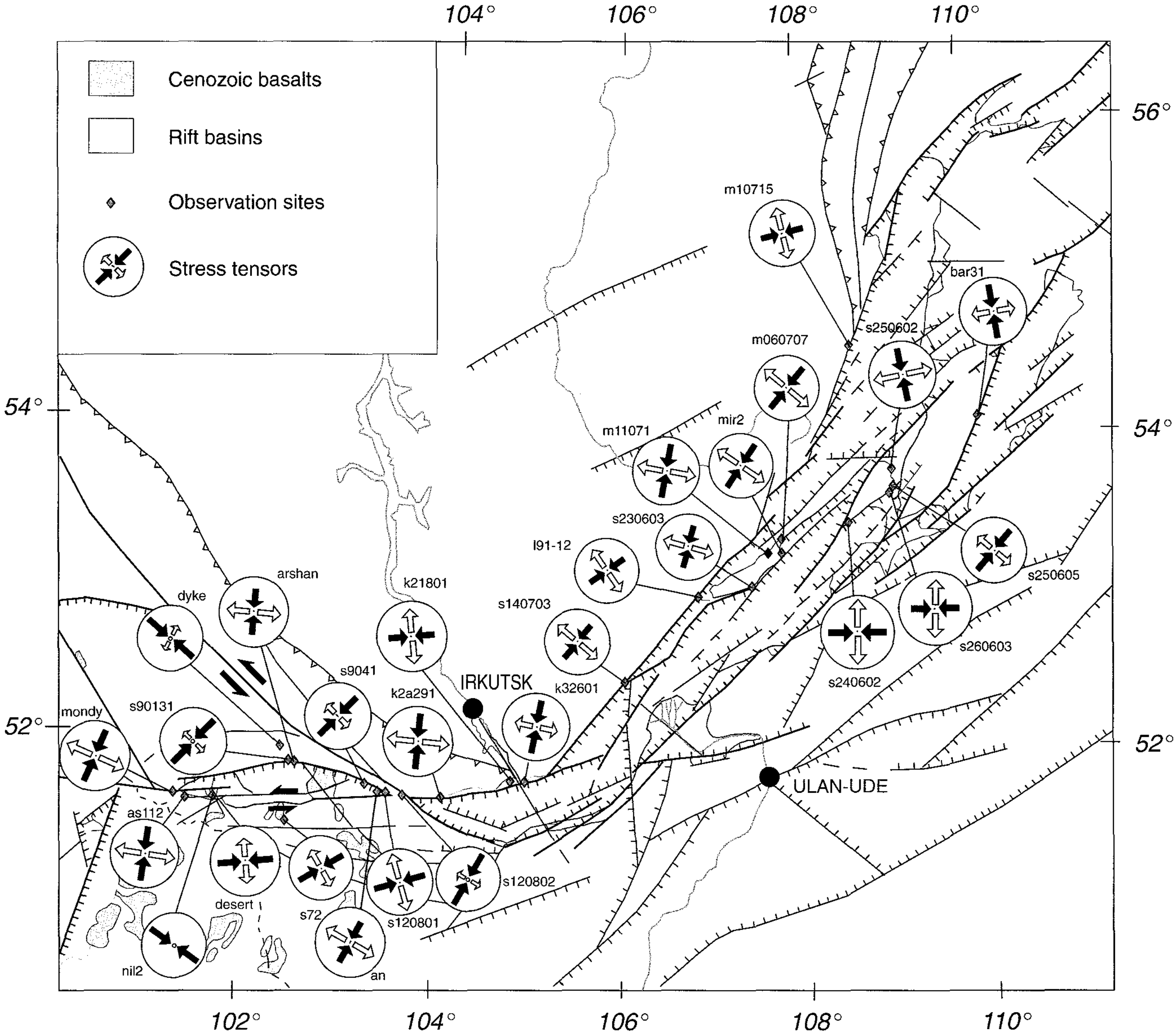

FIGURE 8

Structural map of the BRZ with Cenozoic stress tensors of strike-slip type from fault slip data. Symbols as in Figure 7.

Carte structurale de la zone de rift du Baïkal montrant des tenseurs de contrainte cénozoïque de type décrochant, obtenue à partir des mesures sur les failles cisaillantes. Les symboles sont les mêmes que pour la Figure 7.

FIGURE 7

Structural map of the BRZ with Cenozoic stress tensors of extensional type from fault slip data. Stress symbols with horizontal stress axes (S_{Hmax} and S_{hmin}), in function of the stress ratio R. Their length and colour symbolise the horizontal deviatoric stress magnitude, relative to the isotropic stress (σ_i). White outward arrows: extensional deviatoric stress ($<\sigma_i$). Black inwards arrows: compressional deviatoric stress ($>\sigma_i$). The vertical stress (σ_v) are symbolised by a solid circle for extensional regimes ($\sigma 1=\sigma_v$), a dot for strike-slip regimes ($\sigma 2=\sigma_v$) or an open circle for compressional regimes ($\sigma 3=\sigma_v$).

Carte structurale de la zone de rift du Baïkal montrant des tenseurs de contrainte de type extensif, obtenus à partir des mesures de mouvement des failles. Les symboles représentent les axes de contrainte horizontale (S_{Hmax} and S_{hmin}) en fonction du rapport R des contraintes. Leur longueur et leur couleur symbolisent la valeur du déviateur de contrainte horizontale relatif à la contrainte isotrope (σ_i). Flèches blanches à orientation externe : déviateur de contrainte extensive ($<\sigma_i$). Flèches noires à orientation interne : déviateur de contrainte compressive ($>\sigma_i$). Les contraintes verticales (σ_v) sont représentées par un cercle plein pour les régimes en extension ($\sigma 1=\sigma_v$), par un point pour les régimes décrochants ($\sigma 2=\sigma_v$) et par un cercle pour les régimes en compression ($\sigma 3=\sigma_v$).

population is represented by 27 stress tensors of strike-slip to transpressional regime (Fig. 8). Tensors of transtensional type with S_{hmin} axes trending generally NE-SW to N-S are present in all the studied area of the BRZ. Half of the tensors reconstructed for the Tunka depression have a pure strike-slip to transpressive stress regime, a few of them even show pure compressional stress regime. All these tensors are related to Cenozoic faults.

The preferred orientation of S_{hmin} and S_{Hmax} axes and the mean stress regimes are determined statistically on the diagrams of Figure 9a. For both populations and all stress regimes, the S_{hmin} axis has a relatively stable horizontal position in a NW-SE trend, except for the strike-slip stress regime, for which tensors with N-S trending S_{hmin} axis are relatively frequent. The S_{Hmax} axes have a marked tendency to be oriented in a NNE-trend.

The histogram of distribution of the stress regime index R' shows clearly two well defined maxima (see Fig. 9b). They correspond to the two major populations described above. The population representing the strike-slip stress regime has a maximal frequency of tensors with R' comprised between 1.1 and 1.4 (pure strike-slip with an extensional component), and a tailing distribution of tensors up to R' = 2.0-2.6 (compressional regime). The population representing the extensional regime has a majority of tensors with R' ranging from 0.8 (extension with a strike-slip component) to 0.1 (radial extension), but with most of them of pure extensional type (R' = 0.3 - 0.6).

5. — PRESENT-DAY STRESS FIELD FROM SEISMOTECTONIC DATA

The determination of present-day stress field in the BRZ is based on statistical analysis of earthquake focal mechanism (Solonenko *et al.*, 1997) and on stress inversion of the same data (Petit *et al.*, 1996).

The P and T axes of focal mechanisms compiled by Solonenko *et al.* (1997) are used to construct a schematic map of kinematic axis trajectories in the BRZ (Fig. 10). Only horizontal and inclined (less than 60° from horizontal) P and T axes were used. These trajectories can be regarded as statistical approximations of the S_{hmin} and S_{Hmax} stress trajectories for the current mid- and upper crustal stress field.

In this reconstruction, the trajectories of S_{hmin} generally strike at a high angle (more than 60°) from the trend of the rift basins. The S_{Hmax} trajectories are parallel to the rift structures where they trend N20-60°E, as in the Khubsugul, Baikal, and Barguzin basins. The principal compressive stress axes are horizontal in both extremities of the rift zone, in the Tunka, Kitchera, Upper Angara and Muya basins.

Stress tensor and coefficient $R_1 = (\sigma2 - \sigma1)/(\sigma3 - \sigma1)$ are calculated by the method of Carey-Gailhardis & Mercier (1987). It has to be noticed that the stress ratio R_1 of Carey-Gailhardis & Mercier (1987) differs from the ratio $R = (\sigma2 - \sigma3)/(\sigma1 - \sigma3)$ of Angelier (1994). They are related to each other by $R = 1 - R_1$.

Estimations are obtained for separate areas of the BRZ which differ in terms of quasi-homogeneity of focal mechanisms (Fig. 10). The chosen areas comprise the Kitchera basin and a part of the Upper Angara basin (1), the Barguzin ridge (2), the Barguzin basin (3), the Sviatoy-Nos peninsula (4), the Central Baikal basin (5), the South Baikal basin (6) and the Tunka basin (7). Besides the data homogeneity, the choice of areas was also determined by the availability of focal mechanism data.

As opposed to Petit *et al.* (1996) who used also CMT solutions for strong shocks, we used only data from Russian seismologists (Solonenko *et al.*, 1997), computed from the regional seismic network. Our results are close to the ones of Petit *et al.* (1996), taking into account the relation between R_1 and R.

The results of stress tensor inversion from focal mechanisms show that most part of the BRZ presently develops in conditions of pure extension with R (and R') values close to 0,5 (areas 1, 2, 3, 4, 6 in Fig. 10). A modification of the stress state from pure extension to transpression is evidenced for the Central Baikal basin (area 5), with R (and R') values up to 0,65. For the Tunka area, we did not take into account mechanisms of earthquakes with epicentres located more than 20 km from the Tunka depression. The crust under the Tunka depression is characterized by a transpressional stress regime with R' value of 1.67 (R=0.33, vertical σ2 axis).

As shown by Delvaux (1994), Solonenko *et al.* (1994) and Petit *et al.* (1996), the stress regime is compressional to strike-slip in the area surrounding the BRZ, in Altai and Mongolia to the SW and in the Stanovoy uplift to the NE. The change in stress regime from pure extensional in the central part of the rift zone to transtensional in both flanks and to compressional outside the rift zone can be regarded as a result of the superposition of locally generated extensional stress field over plate-scale compressive stress field.

6. — STRESS FIELD EVOLUTION DURING CENOZOIC

The characteristics of the paleo- and present-day tectonic stress field in the BRZ can be interpreted in terms of Cenozoic stress field fluctuations. Despite the diversity of stress tensors, the σ3 axis is subhorizontal and S_{hmin} is trending NW over most of the investigated part of the BRZ. The changes of S_{hmin} direction from a N-S trend in the southwestern part of the rift zone to a NW-SE trend further north occurs simultaneously with the evolution of the general trend of rift and pre-rift structures. Therefore, the S_{hmin} direction may be influenced by the strike of the regional pre-rift structural pattern.

The distribution of stress regime in time and space in the BRZ suggests that the stress regime changed with time, at least for the Baikal, Barguzin and Kitchera basins: strike-slip paleostress tensors were reconstructed for all the BRZ and the present-day stress field is mainly extensional with exception of the Tunka basin where it is still strike-slip. The same conclusion can be made from the analysis of folding deformations in the seismic profiles of the southern Baikal basin: the upper unit (Middle Pleistocene-Holocene) is not affected by compressional deformation, unlike the intermediate unit (Late Pliocene-Early Pleistocene).

This brings a new question: did the regime of crustal deformation changed with time in the entire territory of the BRZ or has it changed only in the central part of the rift? Logatchev (1993) showed that the rift zone grew from a central point located in the Central Baikal basin. Since the Oligocene, the rift zone flanks became subjected to deformation. The regime of

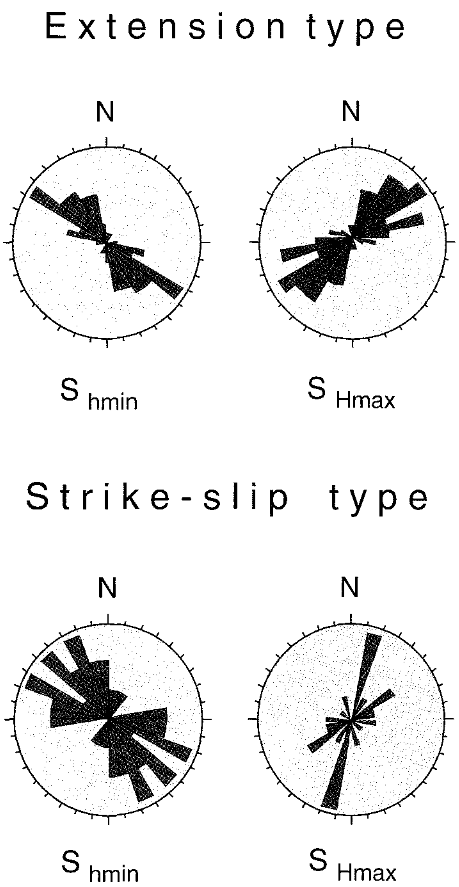

FIGURE 9a

Rose diagrams of S_{hmin} and S_{Hmax} for stress-tensors of extension and strike-slip types in the Baikal rift zone.

Rosaces des S_{hmin} and S_{Hmax} de tenseurs de contrainte de type extension et cisaillement dans la zone de rift du Baïkal.

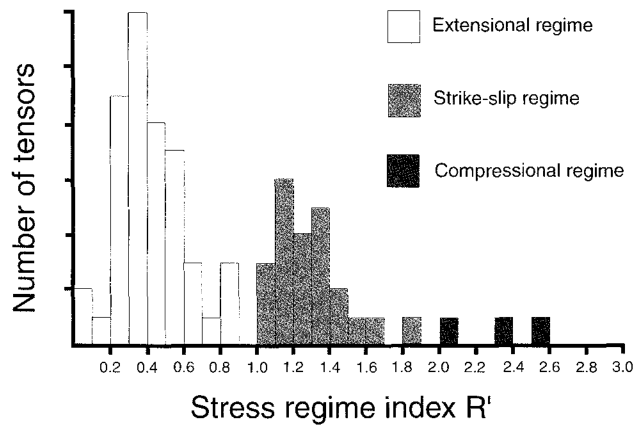

FIGURE 9b

Bar diagram showing the stress regime index R' in function of the number of data used in stress inversion.

Histogramme représentant l'indice R' de régime de contrainte en fonction du nombre de mesures utilisées dans l'inversion de la contrainte.

crustal deformation gradually changed from strike-slip to extensional. The sharp increase in the rate of vertical movements in the Upper Pliocene showed by LOGATCHEV & FLORENSOV (1978) and LOGATCHEV (1993) corresponds to the transition between the two rifting stages. According to the data presented above, we believe that the early stage of rifting is dominated by a strike-slip stress regime and the last stage of rifting is characterized by an extensional stress regime.

The situation in the Tunka basin appears more complex. Tensors of different stress regimes occur close to each other. The paleostress data from dated sediments and volcanics indicate a change in stress state from a strike-slip regime to an extensional regime with time. However, the stress tensors inverted from focal mechanisms show that both systems are presently active. This complex situation in the Tunka area may be the consequence of its location between the rift-type extensional structures of the central part of the Baikal rift and the plate-scale compressional structures of Altai-Sayan and Mongolia. It may be also influenced by the general E-W trend of the Tunka depression which is less favourable for opening than the NE-SW trending Baikal basin.

7. — DISCUSSION

When considering the regional stress field responsible for the formation of tectonic structures, it is important to conduct large-scale investigations over an area which is wider than the object to be studied.

TAPPONNIER & MOLNAR (1979) postulated that neotectonic movements in Central Asia, including the territory of the BRZ, are caused by India-Asia collision. The same conclusion was reached by COBBOLD & DAVY (1988) after confronting modelling results with geological data. However, the stability of present-day S_{Hmax} directions in the upper crust from the Himalaya to the Baikal rift is not by itself a proof of the causal relation between collision and rifting. We believe that the India-Eurasia collision induced neotectonic activations over large territories. The collision is responsible for the formation of the Central Asian mountain belts and the activation of strike-slip zones in Western and Eastern Mongolia, and also reactivation of the southern margin of the Siberian Craton. The formation of extensional structures like the Baikal rift zone may be related to asthenospheric convective flows and mantle diapirism inducing crustal spreading, as suggested by LOGATCHEV & ZORIN (1987). Our resulting data rather suggest a mechanism involving the superposition of plate-scale tectonic forces with NE-trending S_{Hmax} and extensional forces generated by a mantle diapir rising beneath the southeastern boundary of the Siberian Craton.

In spite of the methodological limitation, the fault kinematic and the focal mechanism data used for reconstructing the crustal stress field, allow to characterise the paleo- and present-day stress fields and their variation in time. They also allow to precise the kinematics of movements along the major faults at different geological stages.

In conclusion, a regular evolution of the stress field from a strike-slip regime in the initial stage of rifting to a pure extensional regime in the Quaternary is evidenced for the BRZ. The

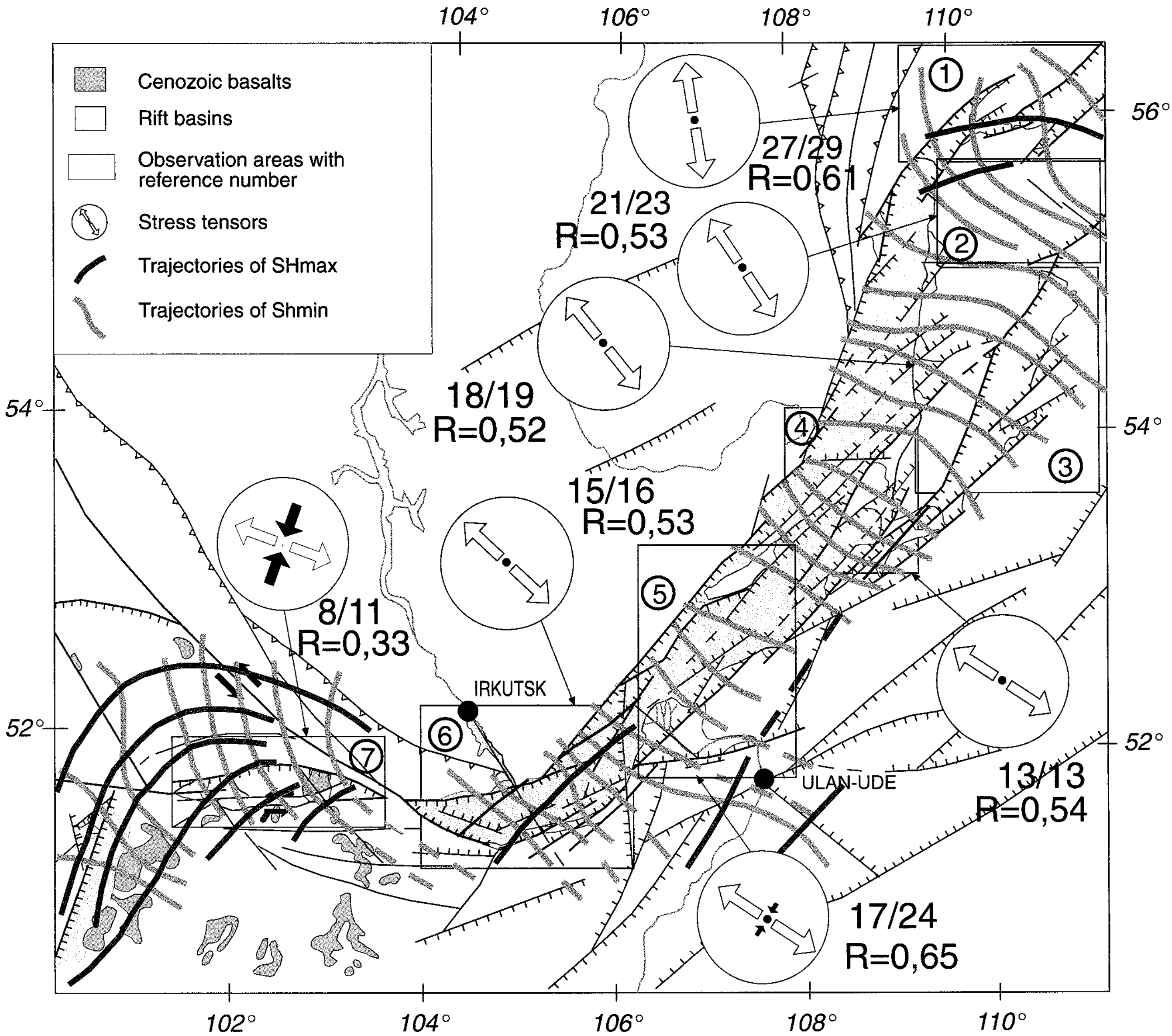

FIGURE 10

Map of present day stress field in the Baikal rift zone. Symbols as in Figure 7. Stress tensors computed from focal mechanism data, using the CAREY-GAILHARDIS & MERCIER (1987) method, but represented with $R = 1 - R_1$, to allow comparison with the tensors computed from fault-slip data.

Carte du champ de contrainte actuel dans la zone de rift du Baïkal. Symboles comme pour la Figure 7. Les tenseurs de contrainte sont calculés à partir des données des mécanismes au foyer en utilisant la méthode de CAREY-GAILHARDIS & MERCIER (1987) mais représentés avec $R = 1 - R_1$, pour permettre la comparaison avec les tenseurs calculés à partir des données sur les failles cisaillantes.

S_{hmin} direction remained stable in a NW-SE direction during all this evolution. The southwestern flank of the BRZ marks the transition from the extensional stress field typical for the rift zone, to the compressional stress field of Mongolia and Altai.

From the different models proposed for the opening of the Baikal rift zone (SHERMAN & LEVI, 1977; ZONENSHAIN & SAVOSTIN, 1978; BALLA *et al.*, 1990), many did not take into account the evolution of crustal stress field with time during rifting. The data presented above highlight the importance of the evolution of rifting dynamics with time. They also confirm the two-stage evolution model proposed on the basis of paleogeographic observations.

This work has been done within the Continental Analysis of Sediment Infill Mechanism project (CASIMIR), with financial support of INTAS (Grant No.93-0134). The authors are grateful to Academician N.A. LOGATCHEV for his support of the investigation data and useful discussions, and to Prof. J. KLERKX for his efforts on the project's organisation and planning of the Russian-Belgian investigations. Co-operation with Dr. J. DÉVERCHÈRE for the seismotectonic part was greatly appreciated. A particular gratitude is expressed to Ms. O.A. BAKSHEEVA and Ms. T.V. LESHKEVICH for the translation of this article into English. This article is part of the special series "Recent Developments in the Geological Knowledge of the Baikal Rift System", edited by N.A. LOGATCHEV and D. DELVAUX and by R. CURNELLE, Chief Editor of the "Bulletin du Centre de Recherches Elf Exploration Production". It is also a contribution to the IGCP 400 project "Geodynamics of Continental Rifting".

8. — REFERENCES

ANGELIER, J. (1989). — From orientation to magnitudes in paleostress determinations using fault slip data. — *J. Struct. Geol.,* **11**, 37-50.

ANGELIER, J. (1994). — Fault slip analysis and paleostress reconstruction. — *In*: HANCOCK, P.L.(ed.): Continental Deformation. — Pergamon, Oxford , 101-120.

ANGELIER, J. & MECHLER, P. (1977). — Sur une méthode graphique de recherche des contraintes principales également utilisable en tectonique et en séismologie : la méthode des dièdres droits. — *Bull. Soc. géol. France,* (7) **19**, 6, 1309-1318.

BALLA, Z., KUZMIN, M. & LEVI, K.G. (1990). — Kinematics of the Baikal rift opening. — *Geotectonics*, **24**,2, 155-164.

BOTT, M.H.P. (1959). — The mechanisms of oblique slip faulting. — *Geol. Mag.,* **96**, 109-117.

CAREY-GAILHARDIS, E. & MERCIER, J.-L. (1987). — A numerical method for determining the state of stress using focal mechanisms of earthquake populations: application to Tibetan teleseisms and microseismicity of southern Peru. — *Earth and Planet. Sci. Lett.,* **82**, 165-179.

CHIPIZUBOV, A.V., SMEKALIN, O.P., BELOUSOV, O.V., DELIANSKY, E.A. & ZSHEGOLEV, YU.V. (1994). — The reverse and strike-slip paleoseismodislocations along Main Sayan Fault zone. — *Dokl. Akad. Nauk* , **338**, 5, 672-674 (in Russian).

COBBOLD, P.R. & DAVY, P. (1988). — Indentation tectonics in nature and experiment. 2. Central Asia. — *Bull. geol. Inst.Univ. Uppsala,* n.s., **14**, 143-162.

DELVAUX, D. (1993). — The TENSOR program for reconstruction: examples from the East African and Baikal rift zones. — *In*: Terra Abstracts, Abstr. suppl. N°1 to *Terra Nova*, **5**, 216.

DELVAUX, D. (1994). — Tectonic control of the paleolimnological evolution of the Baikal rift zone: evidence from paleostress reconstructions. — *In*: Proceedings of the INTAS-SB RAS symposium "Baikal as a Natural Laboratory for Global Change", May 11-17, 1994. — Irkutsk, Russia. Abstr., **4**, 5-6.

DELVAUX, D., MOEYS, R., STAPEL, G., MELNIKOV, A. & ERMIKOV, V. (1995). — Paleostress reconstructions and geodynamics of the Baikal region, Central Asia. Part I: Paleozoic and Mesozoic pre-rift evolution. — *In*: CLOETINGH, S., D'ARGENIO, B., CATALANO, R., HORVATH, H. & SASSI, W.(eds.): Interplay of extension and compression in basin formation. — *Tectonophysics,* spec. Issue, **252**, 61-101.

DELVAUX, D., MOEYS, R., STAPEL, G., PETIT, C., LEVI, K., MIROSHNICHENKO, A., RUZHICH, V. & SAN'KOV, V. (1997). — Paleostress reconstructions and geodynamics of the Baikal region, Central Asia. Part II: Cenozoic rifting. — *Tectonophysics* (in press).

DÉVERCHÈRE, J., HOUDRY, F., SOLONENKO, N.V., SOLONENKO A.V. & SAN'KOV, V.A. (1993). — Seismicity, active faults and stress fields of the North Muya region, Baikal rift: New insights on the rheology of extended continental lithosphere. — *J. Geophys. Res.,* **98**, B11, 19895-19912.

DNEPROVSKY, YU.I. & SAN'KOV, V.A. (1992). — Stress field types of the Baikal rift zone. — 29th Intern. Geol. Congress, Kyoto, Japan (24 August - 3 September 1992), Abstr., **1**, 127.

DOSER, D.I. (1991). — Faulting within the Eastern Baikal rift as characterized by earthquake studies. — *Tectonophysics,* **196**, 109-139.

DUNNE, W.M. & HANCOCK, P.L. (1994). — Paleostress analysis of small-scale brittle structures. — *In*: HANCOCK, P.L. (ed.) : Continental Deformation. — Pergamon, Oxford, 101-120.

FLORENSOV, N.A. (1964). — The Cenozoic tectonics. — *Geology of the USSR*, Nedra, Moscow, **35**, 1, 539-573 (in Russian).

GUIRAUD, M., LABORDE, O. & PHILIP, H. (1989). — Characterization of various types of deformation and their corresponding deviatoric stress tensor using microfault analysis. — *Tectonophysics*, **170**, 289-316.

GZOVSKY, M.V. (1975). — Fundamentals of tectonophysics. — Nauka, Moscow, 533pp. (in Russian).

HUTCHINSON, D.R., GOLMSHTOK, A.J., ZONENSHAIN, L.P., MOORE, T.C., SCHOLZ, C.A. & KLITGORD, K.D. (1992). — Deposition and tectonic framework of the rift basins of Lake Baikal from multichannel seismic data. — *Geology*, **20**, 589-592.

KASHIK, S. A. & MAZILOV, V.N. (1994). — Main stages and paleogeography of Cenozoic sedimentation in the Baikal Rift System (Eastern Siberia). — *Bull. Centres Rech. Explor.-Prod. Elf Aquitaine*, **18**, 2, 453-461.

KULCHITSKY, A.A. (1992). — The rate of Upper Pleistocene sedimentations infilling of Upper Angara and Muya-Kuanda basins of Baikal rift zone. — *Dokl. Acad. Nauk*, **320**, 4, 941-945 (in Russian).

LEVI, K.G., MIROSHNICHENKO, A.I., SAN'KOV, V.A., BABUSHKIN, S.M., LARKIN, G.V., BADARDINOV, A.A., WONG, H.K., COLEMAN, S.& DELVAUX, D. (1997). — Active faults of the Baikal basin. — *Bull. Centre Rech. Elf Explor. Prod.* **21**, 2, 399-434.

LOGATCHEV, N.A. (1993). — History and geodynamics of the Baikal rift in the context of the Eastern Siberia rift system: a review. — *Bull. Centres Rech. Explor.-Prod. Elf Aquitaine,* **17**, 2, 353-370

LOGATCHEV, N.A., ANTOSHCHENKO-OLENEV, I.V., BAZAROV, D.B., GALKIN, V.I., GOLDYREV,G.S., ENDRIKHINSKY, A.S., ZOLOTAREV, A.G., SIZIKOV, A.M. & UFIMTSEV, G.T. (1974). — Pribaikalye and Transbaikalye Highlands. — Nauka, Moscow, 359 pp. (in Russian).

LOGATCHEV, N.A. & FLORENSOV, N.A. (1978). — The Baikal system of rift valleys. — *Tectonophysics*, **45**, 1-13.

LOGATCHEV, N.A. & ZORIN, YU.A. (1987). — Evidence and causes of the two-stage development of the Baikal rift. — *Tectonophysics*, **143**, 225-234.

MILANOVSKY, E.E. (1976). — Rift zones of continents. — Nedra, Moscow, 297 pp. (in Russian).

MISHARINA, L.A. (1964). — To the problem of stresses in earthquake foci of Pribaikalie and Mongolia. — Problems of seismicity of Siberia. — Publishing House of Siberian Branch of the USSR Acad. Sci., 50-69 (in Russian).

MISHARINA, L.A. (1972). — Stresses in earthquake foci of the Mongol-Baikal folded zone. — *In*: SOLONENKO, V.R. (ed.): The field of elastic stresses and earthquake mechanism. — *Seismology*, **8**, 161-171 (in Russian).

MISHARINA, L.A., MELNIKOVA, V.I. & BALGINNJAM, I. (1983). — The south-western boundary of the Baikal rift zone from the data on earthquake focal mechanism — *Volcanology and Seismology*, **2**, 74-83 (in Russian).

MISHARINA, L.A. & SOLONENKO, N.V. (1977). — Earthquake focal mechanism and the stressed state of the Earth's crust in the

Baikal rift zone. — *In*: LOGATCHEV, N.A.(ed.): The role of rifting in the earth's geological history. — Nauka, Novosibirsk, 120-125 (in Russian).

MISHARINA, L.A. & SOLONENKO, N.V. (1981a). — Earthquake focal mechanism in south-eastern flank of the Baikal zone. — *In*: ROGOZHINA, V.A. (ed.): Seismic studies in East Siberia. — Nauka, Moscow, 3-11 (in Russian).

MISHARINA, L.A. & SOLONENKO, N.V. (1981b). — Earthquake mechanism and tectonic stress field. — *In*: SOLONENKO, V.P. (ed.): Seismogeology and detailed seismic zoning of Pribaikalia. — Nauka, Novosibirsk, 76-80, 110-113, 142-146 (in Russian).

MISHARINA, L.A., SOLONENKO, A.V., MELNIKOVA, V.I. & SOLONENKO, N.V. (1985). — Stresses and rupture in earthquake foci. — *In*: SOLOVJEV, S.L. (ed.): Geology and seismicity of the BAM zone. Part I - Seismicity. — Nauka, Novosibirsk, 74-121 (in Russian).

NIKOLAEV, P.N. (1977). — Technique of stress analysis. — *Izvestiya vuzov. Geologiya i Razvedka*, **12**, 70-84 (in Russian).

NIKOLAEV, V. (1990). — Cenozoic history of Baikal depression. — *Geotectonica et Metallogenia*, **14**, 4, 339-350.

PETIT, C., DÉVERCHÈRE, J., HOUDRY-LEMONT, F., SAN'KOV, V.A., MELNIKOVA, V.I. & DELVAUX, D. (1996). — Present-day stress field changes along the Baikal rift and tectonic implications. — *Tectonics*, **15**, 10, 1171-1191.

RASSKAZOV, S.V. (1990). — Pliocene-Quaternary thrust in the South of the Oka plateau, Eastern Sayan Mountains. — *Russian Geology and geophysics*, **31**, 5, 134-138.

RASSKAZOV, S.V. (1993). — Magmatism of the Baikal rift system. — Nauka, Novosibirsk, 285 pp. (in Russian).

RUZHICH, V.V .(1972). — On the problem of dynamics of development of the Earth's crust of Pribaikalie in Cenozoic. — *Geologia i Geofizica*, **4**, 26-32 (in Russian).

RUZHICH, V.V., SHERMAN, S.I. & TARASEVICH, S.I. (1972). — New data on thrusts faults in the south-western Baikal Rift System. — *Doklady, Trans. Acad. Sci. USSR*, Earth science, **205**, 1-6, 68-71.

SAN'KOV, V.A. & DNEPROVSKY, YU.I. (1987). — Fields of strike-slip tectonic stresses and Cenozoic thrusts in the Baikal rift zone. — The Cenozoic geology of the southern East Siberia. Abstracts, Irkutsk, 8. (in Russian).

SAN'KOV, V.A., DNEPROVSKY, YU.I., KOVALENKO, S.N., BORNIAKOV, S.A., GILEVA, N.A., GORBUNOVA, N.G. (1991). — Faults and seismicity of the North-Muya geodynamic testing ground. — Nauka, Novosibirsk, 111 pp. (in Russian).

SHERMAN, S.I. (1992). — Faults and tectonic stresses of the Baikal rift zone. — *Tectonophysics*, **208**, 297-307.

SHERMAN, S.I. & DNEPROVSKY, YU.I. (1986). — New map of stress fields of the Baikal rift zone from geological and structural data. — *Doklady AN SSSR*, **287**, 4, 943-947 (in Russian).

SHERMAN, S.I. & DNEPROVSKY, YU.I. (1989). — Stress fields of the earth's crust and geostructural methods of their investigation. — Nauka, Novosibirsk, 157 pp. (in Russian).

SHERMAN, S.I. & LEVI, K.G. (1977). — Transform faults of the Baikal rift zone. — *Transactions (Doklady) of the USSR Academy of Sciences*, **233**, 1-6, 79-82 (in English).

SHERMAN, S.I., LEVI, K.G., RUZHICH, V.V., SAN'KOV, V.A., DNEPROVSKY, YU.I. & RASSKAZOV, S.V. (1984). — *In*: LOGATCHEV, N.A. (ed.): Geology and seismicity of the Baikal-Amur railway. Neotectonics. — Nauka, Novosibirsk, 206 pp. (in Russian).

SOLONENKO, A.V. (1993). — Symmetry of the crustal stress field in the Baikal rift zone. — *Doklady, Trans. Russian. Acad. Sci.*, Earth science, **330**, 4, 53-57 (in English).

SOLONENKO, A.V., SOLONENKO, N.V., MELNIKOVA, V.I. & SHTEIMAN, E.A. (1997). — The seismicity and earthquake focal mechanisms of the Baikal seismic zone. — *Bull. Centre Rech. Elf Explor. Prod.*, **21**, 1 , 207-231.

SOLONENKO, A.V., SAN'KOV, V.A., SOLONENKO, N.V., MIROSHNICHENKO, A.I. & MELNIKOVA, V.I. (1994). — Spatial and temporal changes in the state of stress of the Baikal rift zone. — *In*: Proceedings of the INTAS-SB RAS symposium "Baikal as a Natural Laboratory for Global Change", May 11-17, 1994, Irkutsk, Russia. Abstr., 4, 43-44.

TAPPONNIER, P. & MOLNAR, P. (1979). — Active faulting and Cenozoic tectonics of the Tian Shan, Mongolia and Baikal regions. — *J. Geophys. Res.*, **84**, B7, 3425-3459.

UFIMTSEV, G.F. (1996). — Soft sediments in process of deformation: example from Baikal rift zone. — *Dokl. Akad. Nauk*, **351**, 4, 517-520 (in Russian).

VISLAVNICH, N.A. (1982). — Evolution of stress field in the structure of Baikal rift: Example from Angara-Muya link uplift. — *In*: Neotectonics and recent dynamics of the lithosphere. Abstracts. — *Tallin*, **1**, 21-22 (in Russian).

VON HAUGWITZ, W.R., WONG, H.K., LEVI, K.G., MATS, V.D. & NIKOLAEV, V.G., (in press). — Late Cenozoic tectonic regime of southern and central Lake Baikal.

VOROPINOV, V.S. (1961). — Gravitational and disjunctive dislocations in the Tertiary deposits at the Lake Baikal bottom along the south-eastern coast. — *In*: The materials on geology of the Mesocenozoic deposits of the Eastern Siberia, Irkutsk, **3**, 26-34 (in Russian).

VVENDENSKAYA, A.V. & BALAKINA, L.M. (1960). — Procedure and results of determination of stresses acting in earthquakes in Pribaikalia and Mongolia. — *Bull. soveta po seismologii*, **10**, 73-84 (in Russian).

ZOBACK, M.L. (1992). — First- and second-order patterns of stress in the lithosphere: the World Stress Map project. — *J. Geophys. Res.*, **97**, 11703-11728.

ZONENSHAIN, L.P. & SAVOSTIN, L.A. (1981). — Geodynamics of the Baikal rift zone and plate tectonics of Asia.— *Tectonophysics*, **76**, 1-2, 1-45.

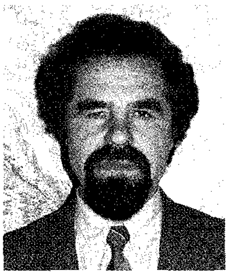

Vladimir Anatolievich SAN'KOV holds a degree in geology from the Irkutsk State University (1978) and a doctorate in geology and mineralogy from the Institute of Geology, Geophysics and Mineralogy in Novosibirsk (1985). In 1988, he became the Scientific Secretary of the Institute of the Earth's Crust for the Siberian Branch of the Russian Academy of Sciences. Since 1997, he has been a Senior Researcher at the Laboratory of Recent Geodynamics. His main scientific interests focus on the study of recent geodynamics stress field, GPS geodesy, and the relationship between fault and seismicity. He is an associate researcher with the Laboratoire de Géodynamique sous-marine de l'Université Paris VI at Villefranche-sur-Mer, the Institut de Géodynamique de l'Université de Nice – Sofia Antipolis, France and the Musée Royal de l'Afrique Centrale, Tervuren, Belgium.

Vladimir Anatolievich SAN'KOV a acquis sa licence de géologie à l'Université d'État d'Irkoutsk en 1978, et son doctorat en géologie et minéralogie à l'Institut de Géologie, Géophysique et Minéralogie de Novossibirsk en 1985. En 1988, il est devenu secrétaire scientifique de l'Institut de la Croûte Terrestre de la Section Sibérie de l'Académie des Sciences de Russie. Depuis 1997, il est maître de recherches au Laboratoire de géodynamique actuelle. Ses principales recherches portent sur le champ de contrainte en géodynamique, la géodésie par GPS et le rapport entre failles et sismicité. Il est chercheur associé du Laboratoire de Géodynamique sous-marine de l'Université Paris VI à Villefranche-sur-mer, de l'Institut de Géodynamique de l'Université de Nice - Sofia Antipolis, France et du Musée Royal de l'Afrique Centrale, Tervuren, Belgique.

Andrei Ivanovich MIROSHNICHENKO graduated with a degree in geology from the State University of Irkutsk (1976) and a doctorate in geology and mineralogy from the Institute of Geology, Geophysics and Mineralogy in Novosibirsk (1989). In 1997, he became a Senior Researcher at the Laboratory of Recent Geodynamics at the Institute of the Earth's Crust for the Siberian Branch of the Russian Academy of Sciences. He studies deformation and block movements, faulting and stress field. He is an associate researcher with the Laboratoire de Géodynamique sous-marine de l'Université Paris VI at Villefranche-sur-Mer, the Institut de Géodynamique de l'Université de Nice – Sofia Antipolis, France and the Musée Royal de l'Afrique Centrale, Tervuren, Belgium.

Andrei Ivanovich MIROSHNICHENKO a obtenu sa licence de géologie à l'Université d'État d'Irkoutsk en 1976, et son doctorat en géologie et minéralogie à l'Institut de Géologie, Géophysique et Minéralogie de Novossibirsk en 1989. En 1997, il est devenu maître de recherches au Laboratoire de géodynamique actuelle à l'Institut de la Croûte Terrestre de la Section Sibérie de l'Académie des Sciences de Russie. Il étudie la déformation et les mouvements des blocs, la formation des failles et les champs de contrainte. Il est chercheur associé du Laboratoire de Géodynamique sous-marine de l'Université Paris VI à Villefranche-sur-mer, de l'Institut de Géodynamique de l'Université de Nice - Sofia Antipolis, France et du Musée Royal de l'Afrique Centrale, Tervuren, Belgique.

Kirill Georgievich LEVI obtained a geomorphology degree from the Irkutsk State University in 1974 and a doctorate in geology and mineralogy from the Institute of Geology, Geophysics and Mineralogy, Novosibirsk in 1981. In 1991, he became the Deputy Director of the Institute of the Earth's Crust for the Siberian Branch of the Russian Academy of Sciences. Since 1998, he has been head of Laboratory of Recent Geodynamics. His research activities include neotectonics, recent geodynamics, crustal movements, seismic hazard and risk. He is an associate researcher with the Laboratoire de Géodynamique sous-marine de l'Université Paris VI at Villefranche-sur-Mer, the Institut de Géodynamique de l'Université de Nice – Sofia Antipolis, France and the Musée Royal de l'Afrique Centrale , Tervuren, Belgium.

Kirill Georgievich LEVI a acquis sa licence de géomorphologie à l'Université d'État d'Irkoutsk en 1974 et son doctorat en géologie et minéralogie à l'Institut de Géologie, Géophysique et Minéralogie de Novossibirsk en 1981. En 1991, il est devenu sous-directeur de l'Institut de la Croûte Terrestre de la Section Sibérie de l'Académie des Sciences de Russie. Depuis 1998, il est chef du Laboratoire de Géodynamique actuelle. Il fait des recherches sur la néotectonique, les mouvements de la croûte terrestre et les risques sismiques. Il est chercheur associé du Laboratoire de Géodynamique sous-marine de l'Université Paris VI à Villefranche-sur-mer, de l'Institut de Géodynamique de l'Université de Nice - Sofia Antipolis, France et du Musée Royal de l'Afrique Centrale, Tervuren, Belgique.

Andrei Victorovich LUKHNEV holds a degree in geology from the State University of Irkutsk (1993). In 1997, he became a Researcher for the Laboratory of Recent Geodynamics at the Institute of the Earth's Crust for the Siberian Branch of the Russian Academy of Sciences. He studies recent geodynamics, GPS geodesy, and fault kinematics. He is an associate researcher with the Laboratoire de Géodynamique sous-marine de l'Université Paris VI at Villefranche-sur-Mer and the Institut de Géodynamique de l'Université de Nice – Sofia Antipolis, France.

Andrei Victorovich LUKHNEV a obtenu sa licence de géologie à l'Université d'État d'Irkoutsk en 1993. En 1997, il est devenu chercheur au Laboratoire de Géodynamique actuelle à l'Institut de la Croûte Terrestre de la Section Sibérie de l'Académie des Sciences de Russie. Il fait des recherches sur la géodynamique actuelle, la géodésie par GPS et la cinématique des failles. Il est chercheur associé du Laboratoire de Géodynamique sous-marine de l'Université Paris VI à Villefranche-sur-mer et de l'Institut de Géodynamique de l'Université de Nice - Sofia Antipolis, France.

Alexander Ivanovich Melnikov obtained a degree in geology from the State University of Irkutsk in 1972 and a doctorate in geology and mineralogy from the Institute of the Earth's Crust in Irkutsk in 1983. In 1988, he became a Senior Researcher at the Paleogeodynamics Laboratory at the Institute of the Earth's Crust for the Siberian Branch of the Russian Academy of Sciences. His main scientific interests include structural geology, geotectonics, tectonophysics. He is an associate researcher with the Musée Royal de l'Afrique Centrale, Tervuren, Belgium.

Alexandre Ivanovich Melnikov a obtenu sa licence de géologie à l'Université d'État d'Irkoutsk en 1972 et son doctorat de géologie et minéralogie à l'Institut de la Croûte Terrestre d'Irkoutsk en 1983. En 1988, il est devenu maître de recherches au Laboratoire de Paléogéodynamique de l'Institut de la Croûte Terrestre de la Section Sibérie de l'Académie des Sciences de Russie.Ses sujets de recherche sont la géologie structurale, la géotectonique et la tectonophysique. Il est chercheur associé du Musée Royal de l'Afrique Centrale, Tervuren, Belgique.

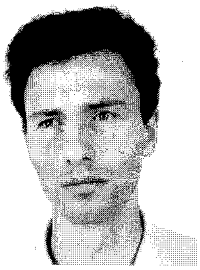

Damien Delvaux obtained a degree in geology and mineralogy from the University of Louvain-La-Neuve (Belgium), in 1980. After one year of geological mapping in Belgium and four years in the Geochemistry Laboratory of the Petrofina oil and gas company, he received his doctorate in geology and mineralogy from the University of Louvain-la-Neuve in 1988. Since 1989, he has been assistant-researcher at the Department of Geology and Mineralogy of the Royal Museum for Central Africa. He is involved in the investigation of rifting processes in the Tanganyika and Malawi rift systems, and their comparison with the Baikal Rift System. He focuses mainly on the tectonic control of sedimentary basin formation, neotectonics and active tectonic processes.

Damien Delvaux a obtenu sa licence en géologie et minéralogie à l'Université de Louvain-la-Neuve (Belgique), en 1980. Après une année de cartographie géologique en Belgique et quatre années au Laboratoire de Géochimie de la compagnie pétrolière Petrofina, il a acquis son doctorat en géologie et minéralogie à l'Université de Louvain-la-Neuve, en 1988. Depuis 1989, il est chercheur-assistant au Département de Géologie et Minéralogie du Musée Royal de l'Afrique Centrale. Il est impliqué dans des recherches sur les processus de riftogenèse dans les rifts de Tanganyika et Malawi, et leur comparaison avec le système de rift du Baïkal. Ses principaux sujets de recherche sont le contrôle tectonique des bassins sédimentaires, la néotectonique et la tectonique active.

APPENDICES 1 et 2

APPENDIX 1

Paleostress tensors from fault-slip data.

Tenseurs de paléocontrainte obtenus à partir des mesures sur les failles cisaillantes.

Site	Lat. °N	Long °E	Localisation / lithology	n	nt	σ1	σ2	σ3	R	α	R'
1s121	109.30	55.35	Nijne-Angarsk v., granites	17	57	86/076	03/233	03/313	0.56	10.6	0.56
1s141	102.53	51.42	Right bank Zun-Murin r., gneisses	18	63	56/117	33/199	00/108	0.25	5.8	0.25
2s121	101.44	51.42	Arshan v., Zamaraiha r., gneisses	13	100	69/083	20/240	08/334	0.21	8.9	0.21
60km	107.45	52	60 km route Ulan Ude - Ust Barguzin, gneisses	17	19	69/146	01/055	21/325	0.65	8.1	0.65
Arshan	102.26	51.54	Arshan v., marbles	11		26/015	61/169	11/280	0.73	6.5	1.27
Mondi	100.59	51.35	W Mondy v., left bank Irkut r., conglomerates (Miocene ?)	50	64	10/018	75/145	12/206	0.74	7.3	1.26
as112	101.07	51.40	500 m E Mondy v., left bank Irkut r., marbles	10	10	27/019	56/157	19/279	0.56	0.9	1.44
bar11	108.58	53.22	SW side Barguzin bay, granites	14	27	46/063	32/194	26/302	0.58	9.5	0.58
bar31	110.03	54.02	Barguzin basin, Tun r., granites	18	50	22/345	59/213	20/084	0.55	7.9	1.45
bar32	110.48	54.41	Barguzin basin, Alla r., granites	29	34	69/298	02/035	21/125	0.39	10.8	0.39
desert	101.40	51.39	1 km S Nilova Pustyn v., volcanic rocks (N)	15	38	11/269	79/104	03/359	0.26	10.0	1.74
grab	107.29	53.15	2 km NE Kharantsi c., clay	14	26	62/066	26/222	10/317	0.28	11.7	0.28
k2084	106.30	53.33	left bank Buguldeika r., gneisses	18	60	41/044	49/216	04/311	0.55	10.4	1.45
k21801	104.48	51.53	Port Baikal, marbles	10	22	00/079	65/168	25/350	0.73	8.5	1.27
k2a022	58.14	61.73	Ludar c., gneisses	16	36	69/135	01/044	20/313	0.42	7.5	0.42
k2a031	58.58	66.55	Kurla c., gneisses	17	39	82/070	07/226	03/316	0.02	9.1	0.02
k2a142	106.56	53.01	NE Olkhon Gate, migmatites	21	41	58/260	32/075	03/166	0.52	8.3	0.52
k2a191	107.47	53.24	100 m E Khoboi c., gneisses	25	52	86/286	01/033	04/123	0.01	9.9	0.01
k2a291	104.03	51.45	132 km round Baikal railway Port Baikal-Sludyanka t., migmatites	16	22	04/186	86/357	01/096	0.50	9.2	1.50
k32601	104.50	51.52	Listvianka v., migmatites	17	41	29/199	60/038	08/293	0.71	9.5	1.29
k32602	104.53	51.50	Listvianka c., migmatites	25	44	76/010	13/182	01/272	0.52	10.1	0.52
l91-12	106.55	53.09	Tsagan-Hushun c., Small Sea, clay	9	105	27/063	63/235	03/331	0.72	10.7	1.28
m050706	106.35	52.46	Left bank Anga r., marbles	10	27	43/075	39/296	22/187	0.55	7.9	0.55
m060707	107.46	53.24	400 m W Khoboi c., gneisses	11	26	38/060	51/223	09/323	0.45	7.7	1.55
m070708	108.11	54.01	1 km S Pokoiniki c., schists	12	24	44/025	46/209	02/117	0.38	4.2	0.38
m070709	108.39	51.58	Elokhin c., granites	12	32	50/081	40/260	01/351	0.25	7.6	0.25
m080711	108.54	54.54	Bolsodei c., gneiss	10	25	56/053	33/251	08/155	0.43	10.3	0.43
m080712	109.00	55.01	Kotelnikovski c., migmatites	17	68	73/067	12/031	12/299	0.5	6.4	0.5
m10713	108.47	54.41	1.5 km N Khibilen c., tuff sandstones	17	32	61/022	19/253	21/155	0.8	10.0	0.80
m10714	108.46	54.40	1 km N Khibilen c., tuff sandstones	19	26	53/228	36/029	09/126	0.31	6.0	0.31
m10715	108.45	54.40	0.5 km N Khibilen c., tuff sandstones	20	33	02/078	56/344	33/169	0.87	13.0	1.13
m11071	107.38	53.18	Sasa c., gneisses	8	20	14/014	75/217	06/105	0.65	9.5	1.35
m11716	106.30	52.48	Zunduk c., Centre Baikal, marbles	17	27	52/1789	14/071	34/331	0.35	8.7	0.35
m240603	106.56	52.59	SE Olkhon Gate, gneisses	15	30	69/095	19/248	09/341	0.85	8.3	0.85
m91-12	106.46	53.01	Mukhor bay, Small Sea, gneisses	32	96	63/144	05/244	27/336	0.85	9.7	0.85
mai222	106.48	53.07	Right bank Sarma r., gneisses	14	60	78/359	09/223	08/132	0.33	7.0	0.33
mir2	107.45	53.19	N Olkhon island, Uzur v., marbles	15	113	12/235	77/235	04/124	0.54	8.0	1.46
r41	108.58	53.22	SW side Barguzin bay, granites	60		73/118	07/232	15/324	0.47	8.80	0.47
s120802	103.26	51.47	Anchuk v., right bank r.Irkut, granites	10	10	04/035	05/305	84/163	0.57	0.30	2.57
s140702	106.02	52.33	Right bank Buguldeika r., blastocataclasites	10	14	73/087	17/255	03/346	0.43	9.4	0.43
s210801	102.26	51.54	Arshan v., marbles, basalt dyke (N)	7	50	66/335	05/233	23/141	0.37	0.34	0.37
s140703	106.01	52.31	3 km SW Buguldeika v., mylonites	11	23	23/219	63/073	13/314	0.68	6.7	1.32
s220601	106.30	53.33	1.5 km SW Buguldeika v., blastocataclasites	11	101	50/190	35/044	17/302	0.39	7.7	0.39
s230603	107.18	53.03	SW Olkhon i., Tashkinei r., gneisses	8	35	17/197	65/066	17/293	0.77	4.4	1.23
s230604	107.41	53.13	3 km W Idgimey c., marbles, gneisses	27	61	52/174	01/265	38/357	0.62	10.6	0.62
s240601	108.35	53.31	1.5 km NE Nijne-Izgolovie c., Svyatoi Nos, migmatites	28	82	52/052	36/207	12/306	0.31	12.8	0.31
s240602	108.32	53.30	0.5 km NE Nijne-Izgolovie c., Svyatoi Nos, migmatites	38	102	28/092	62/282	04/148	0.66	8.9	1.34
s250601	108.56	53.51	N Svyatoi Nos, 4 km E Orlov c., marbles	15	87	65/259	22/053	09/147	0.25	6.7	0.25

APPENDIX 1 (cont.)

Site	Lat. °N	Long °E	Localisation / lithology	n	nt	$\sigma 1$	$\sigma 2$	$\sigma 3$	R	α	R'
s250602	109.02	53.49	Chivyrkui bay, E side Molodost, gneisses	42	95	25/343	56/209	21/083	0.46	11.9	1.54
s260601	109.03	53.48	Chivyrkui bay, Fertik c., gneisses	35	73	84/291	02/038	06/128	0.12	9.45	0.12
s260602	109.02	53.47	Chivyrkui bay, Ongononski c., gneisses	28	76	84/229	06/036	01/126	0.29	12.7	0.29
s260603	109.01	53.40	Chivyrkui bay, Kurbulik v., granites	11	104	38/273	60/082	05/180	0.82	6.8	1.18
s260605	109.01	53.41	Chivyrkui bay, 1 km N Kurbulik v., granites	15	43	22/058	54/183	27/316	0.34	9.9	1.66
s270601	109.12	53.49	250 m S Malaia Suhaia r., gneisses	20	64	54/236	32/088	15/348	0.5	8.7	0.50
s270602	109.14	53.51	1 km N s270602, gneisses	11	36	70/279	04/178	20/086	0.81	9.3	0.81
s270603	108.42	53.51	Maloye Ushkany i., Dlini i.,marbles	12	37	59/125	50/287	08/021	0.55	9.0	0.55
s280601	108.38	53.52	Bolshoi Ushkany i., marbles	9	101	73/284	17/107	01/017	0.4	3.0	0.40
s290601	109.52	55.25	Aia bay, marbles	13	52	38/217	38/345	38/101	0.24	11.9	0.24
s300601	107.34	53.33	Kulgana c., Central Baikal, schists	18	62	71/222	16/075	10/342	0.53	11.7	0.53
s71	102.23	51.34	Kharagun r., gneisses	16	100	64/265	08/012	25/105	0.4	5.0	0.40
nil2	101.40	51.39	1 km S Nilova Pustyn v., volkanic rocks (N)	11	68	35/015	19/272	48/158	0.73	14.0	2.73
s90134	102.25	51.54	1.5 km N Arshan v., marbles	11	100	60/052	30/232	00/322	0.5	0.4	0.50
s9041	103.07	51.49	3 km NNW Shimki v., granites	10	100	19/238	65/099	15/333	0.86	1.8	1.14
s9071	103.39	51.44	3km W Kultuk v., gneisses	29	94	66/015	24/195	00/285	0.5	0.3	0.50
sar1	106.49	53.07	Right and left banks Sarma r., gneisses	21	51	73/175	09/051	14/319	0.63	14.5	0.63
shar	103.58	51.44	Sharyzhalgay v., granulites	15	38	83/052	07/216	02/306	0.22	9.3	0.22
s90131	102.26	51.54	Arshan v., marbles	17	101	15/056	10/323	72/199	0.23	0.4	2.23
dyke	103.39	51.46	NW Arshan v., basalt dyke (14 Ma)	20	28	17/307	72/118	03/217	0.08	4.9	2.08
tur	101.43	51.37	1 km Turan v., Pleistocene deposits	39	64	62/270	20/044	18/141	0.24	9.0	0.24
tan	105.14	51.68	Tankhoy v., N deposits	31	64	67/015	23/201	02/110	0.37	4.6	0.37
an	103.24	51.47	Anchuk v., left b. Irkut r., Pliocene deposits	10	20	04/025	79/137	10/294	0.62	11.0	1.38

APPENDIX 2

Stress tensors from earthquakes focal mechanisms. Data source: SOLONENKO *et al.* (1997).

Tenseurs de contrainte obtenus à partir de mécanismes au foyer de tremblements de terre.

Area N°	Lat. °N	Long °E	Area Name	n	nt	$\sigma 1$	$\sigma 2$	$\sigma 3$	R_1	R	R'
1	110.0 112.8	55.7 56.5	Upper Angara and Kitchera basins	27	29	248/84	74/06	344/01	0.39	0.61	0.61
2	110.0 112.5	54.7 55.7	Barguzin ridge	21	23	251/88	34/02	124/01	0.47	0.53	0.53
3	109.9 112.0	53.7 55.0	Barguzin basin	18	19	221/82	49/08	319/01	0.48	0.52	0.52
4	108.0 109.1	53.2 54.1	Svyatoi-Nos peninsula	13	13	166/79	41/06	303/09	0.46	0.54	0.54
5	106.0 108.1	52.0 53.3	Central Baikal basin	17	24	49/73	212/17	303/05	0.35	0.65	0.65
6	104.0 106.0	51.3 52.3	South Baikal basin	15	16	127/74	222/01	313/16	0.47	0.53	0.53
7	101.5 103.5	51.7 52.0	Tunka basin	8	11	199/35	23/54	290/02	0.67	0.33	1.67

n: number of fault data used for stress tensor determination; nt: total number of fault data measured; $\sigma 1$, $\sigma 2$, $\sigma 3$: plunge and azimuth of principal stress axes;

$R_1 = (\sigma 2 - \sigma 1)/(\sigma 3 - \sigma 1)$: Stress ratio of CAREY; $R = (\sigma 2 - \sigma 3)/(\sigma 1 - \sigma 3)$: Stress ratio of ANGELIER; α: mean slip deviation (°); R': stress regime index.

n : nombres de mesures utilisées pour la détermination des tenseurs de contrainte ; nt : nombre total de mesures faites ; $\sigma 1$, $\sigma 2$, $\sigma 3$: inclinaison et azimut des axes de contrainte ;

$R_1 = (\sigma 2 - \sigma 1)/(\sigma 3 - \sigma 1)$: rapport de contrainte de CAREY; $R = (\sigma 2 - \sigma 3)/(\sigma 1 - \sigma 3)$: rapport de contrainte d'ANGELIER ; α : déviation moyenne de cisaillement (°) ; R' : indice régime de contrainte.